

The Effect of the SIT Injection Rate on Delaying RPV Failure during Severe Accidents

Seungwon Seo^a, Hwan-Yeol Kim^b, Kwang Soon Ha^b, Gyoodong Jeun^a, Sung Joong Kim^{a*}

^a Department of Nuclear Engineering, Hanyang University,
 222 Wangsimni-ro, Seongdong-gu, Seoul, 133-791, Korea

^b Severe Accident and PHWR Safety Research Division, Korea Atomic Energy Research Institute,
 1045 Daedeok-daero, Yuseong-gu, Daejeon, 305-353, Republic of Korea

*Corresponding author: sungjkim@hanyang.ac.kr

1. Introduction

Fukushima Daiichi accident shed light on the importance of the safe design and proper operation of a nuclear power plant during the severe accidents. Phenomena on the severe accident are exceptionally hard to be analyzed due to the inherent nature of complexity and uncertainty. Therefore, studies on reducing such complexity and uncertainty have been conducted recently. A great concern is focused on the core coolability in the case of hypothesized severe accidents. In specific, the relationship between entering severe accident management guidance (SAMG) and accompanying reactor pressure vessel (RPV) failure time was analyzed in our previous study. Lee et al. [1] studied the effect of mitigation strategy of three postulated accidents using the MELCOR code.

The objective of this study is to investigate the SAMG entry condition effect on delaying RPV failure. Delayed RPV failure time was measured for postulated scenarios with various SAMG entry conditions. Also mass balance analysis focused on reactor coolant system (RCS) is conducted to investigate safety injection tank (SIT) effect on the RPV failure. Severe accident code MELCOR 1.8.6 was used to simulate and a reference plant is selected as the Korean Pressurized Water Reactor (PWR) Optimized Pressurized Reactor (OPR) 1000.

2. Simulation Descriptions

2.1 MELCOR Input Model of OPR1000

MELCOR is the severe accident analysis code for light water reactor nuclear power plant developed by Sandia National Laboratory for the U.S. Nuclear Regulatory Commission. Probabilistic Safety Assessment (PSA) level 2 analyses, the development and validation of severe accident management strategies are conducted using MELCOR. MELCOR can simulate thermal-hydraulic response of the primary reactor coolant system, core uncovering, fuel heat-up, cladding oxidation, fuel degradation (geometry change), heat-up of RPV lower head by molten core, lower plenum penetration, hydro production, behavior of fission product release, etc. [2]

Fig. 1 shows the overall nodalization of the reference plant OPR1000 for the MELCOR simulation. The input model consists of the core, the pressurizer, four cold-legs, two hot-legs, two steam generators, and so on. The dedicated upper plenum volume for collecting CET

information is allocated to the top of the core. The SITs are activated when RCS pressure decreases to 4.3 MPa. The pressurizer has two safety depressurization system (SDS) valves and a pressure safety relief valve (PSRV) that are all connected to the containment. The SDS is operated as a mitigation strategy under a high pressure sequence for direct RCS depressurization. Set pressures of the PSRV are 17.24 MPa and 14.1 MPa for open and close, respectively. Each steam generator is equipped with two atmospheric dump valves (ADV) and four condenser dump valves (CDVs).

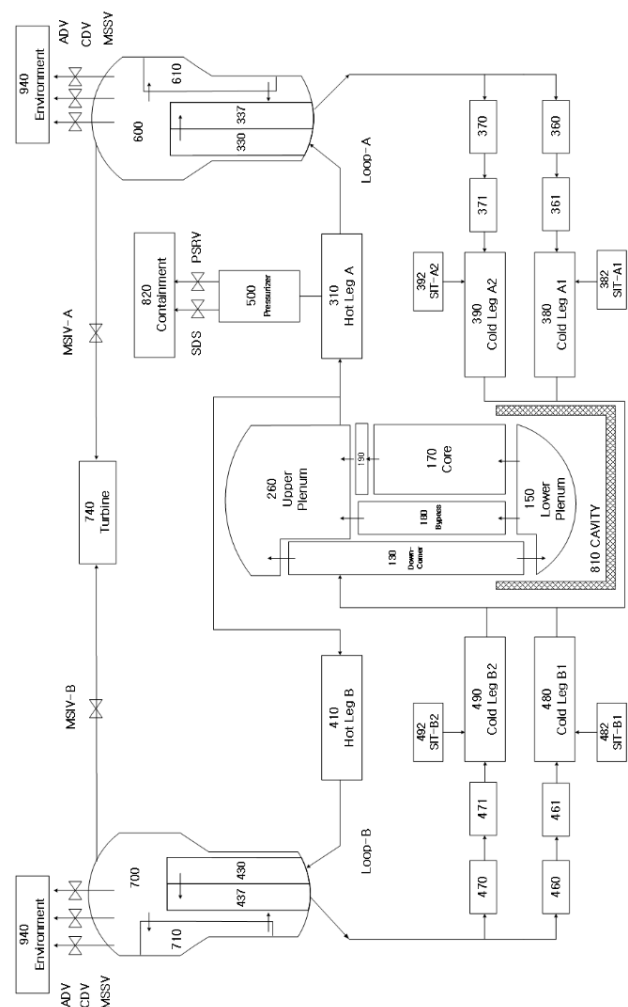


Fig. 1. MELCOR nodalization of OPR1000

2.2 Simulation Matrix and Mitigation Strategy for Accidents

Table I summarizes a matrix for simulations investigated in this work. The Combustion Engineering Owners Group (CEOG), Westinghouse Owners Group (WOG), Framatome, and EDF PWR implement CETs of 753 K, 923 K, 973 K, and 1373 K for SAMG entry conditions, respectively. In order to investigate the effects of various SAMG entry conditions, three cases of initiating events are selected: Small Break Loss of Coolant Accident (SBLOCA), Station Blackout (SBO), and Total Loss of Feed Water (TLOFW). Table II shows initiating events that exhibit a high probability of transition to a severe accident based on the PSA Level 1 analysis [3]. For the SBLOCA, a 1.35-inch break on a cold leg is assumed, and loss of all off-site power and all secondary feed water are assumed for the SBO and TLOFW, respectively. Mitigation-02 is conducted by opening one ADV for the SBLOCA and opening one SDS for the SBO and TLOFW.

In order to adopt mitigating strategies according to the SAMG flow chart of OPR1000, Mitigation-02 is applied for the postulated initiating events. In the case of the SBLOCA, opening the ADV facilitates heat transfer through secondary side feed-and-bleed, which depressurizes the RCS. For the SBO and TLOFW, direct RCS depressurization by opening one SDS of the pressurizer is adopted as a proper mitigation mean. In the case of the SBO, it is assumed that emergency power (emergency diesel generators or DC power) for opening SDS is available. In addition, to be conservative, both High Pressure Safety Injection (HPSI) and Low Pressure Safety Injection (LPSI) are assumed to be unavailable for the TLOFW. Borated water from four SITs with a capacity of 218 m³ is injected into cold legs for all three postulated initiating events if the RCS pressure decreases to 4.3 MPa. The SITs are passive injection methods and are identical to the cold leg accumulators of the WOG PWR.

Table I: Summary of the simulation matrix

Event	Mitigation	CET (SAMG entry condition)	Simulation tag
SBLOCA	OFF	N/A	SBLOCA-Base
SBLOCA	ADV	753, 838, 923 and 973 K	SBLOCA-CET K
SBO	OFF	N/A	SBO-Base
SBO	SDS	753, 838, 923 and 973 K	SBO-CET K
TLOFW	OFF	N/A	TLOFW-Base
TLOFW	SDS	753, 838, 923 and 973 K	TLOFW-CET K

Table II: Probability of transition from initiating events to severe accidents for OPR1000

Initiating event	Probability (%)
SBLOCA without safety injection	22.4
SBO	14.4
TLOFW	13.8
STGR	13.8
LBLOCA without safety injection	12.7
MBLOCA without safety injection	7.7

3. Results and Discussion

3.1. Steady State

Using the current MELCOR simulation, a steady state calculation was performed to verify the suitability of the nodalization of the OPR1000. Nominal operating conditions of the OPR1000 are available in the FSAR [4]. Table III shows a comparison between the operating conditions described in the Final Safety Analysis Report (FSAR) and steady state calculation results of the OPR1000 using MELCOR. It is observed that the MELCOR results are in good agreement with the nominal FSAR values, which confirms the suitability of current MELCOR nodalization.

Table III: Design value and steady state conditions of OPR1000

Parameter	FSAR	MELCOR
Core thermal power (MWt)	2,815	2,815
RCS pressure (MPa)	15.5	15.5
Core inlet temperature (K)	569	573
Core outlet temperature (K)	601	603
Primary flow rate (kg/sec)	15,306	15,546
Secondary side pressure (MPa)	7.37	7.37
Steam flow per SG (kg/sec)	800	809

3.2. Base Cases

A timeline of significant events without mitigation strategies of the base cases is summarized in Table IV, and Fig. 2 shows the RCS pressure of the base cases. All accidents started at time = 0 second, and the reactor was tripped by receiving a signal from the pressurizer for the case of SBLOCA, a power loss signal for the SBO, and a steam generator low water level signal for the TLOFW. Also, the reactor coolant pump tripped due to cavitation for the SBLOCA and TLOFW and power loss for the SBO. For all three base cases, decay and oxidation heat with insufficient core cooling caused the core to be uncovered, heated, and degraded to a molten state. As the core was heated, the CET also increased with a similar rate of increase. As the insufficient cooling continued, the molten core was relocated to the lower plenum. Finally, RPV failure occurred through lower head penetration for the SBLOCA and by creep rupture for the SBO and TLOFW. The RPV failure times of each

initiating event were calculated as 5.29, 3.81, and 2.40 hours for the SBLOCA, SBO, and TLOFW, respectively. For the SBLOCA, SITs were activated after relocation to the lower plenum because the RCS pressure was decreased to the set point of the SIT injection. However, for SBO and TLOFW, injection of the SITs was not actuated because high pressure sequences continued.

Table IV: Sequences of base cases

Accident sequence	SBLOCA (hr)	SBO (hr)	TLOFW (hr)
Accident start	0.00	0.00	0.00
Reactor trip	0.04	0.00	0.01
RCP trip	0.06	0.00	0.42
PSRV open	N/A	1.36	0.40
Time to reach CET = 923 K	2.36	2.27	1.00
Clad melting	2.63	2.66	1.28
Relocation	2.87	2.82	1.48
SIT injection	3.63	N/A	N/A
SIT exhaust	5.37	N/A	N/A
RPV failure	5.29	3.81	2.40

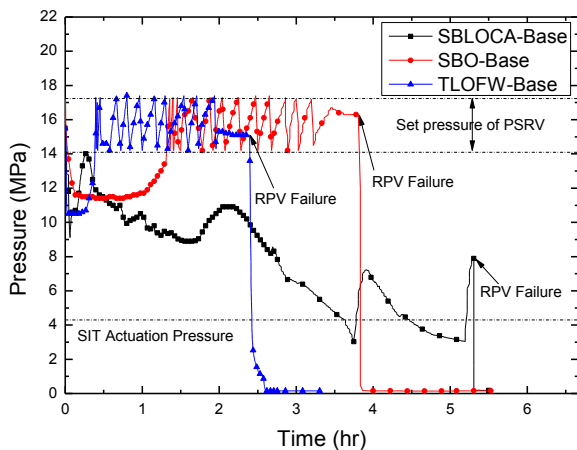


Fig 2. RCS pressure of base cases

3.3 SAMG Entry Condition Effect on In-Vessel Mitigation

The effect of SAMG entry conditions on the RPV failure time was analyzed in terms of the delayed RPV failure time. In addition, mass balance between the core water inventory, injected water, and discharged water was analyzed to investigate the effect of SIT injection on the delay of RPV failure. Figure 6 shows the conceptual diagrams of two types of measured time. Operator's available action time was calculated as the differential time between the time the CET reached the hypothesized SAMG entry conditions and the RPV failure time of the base cases. Delayed RPV failure time was measured as the time between the onset of RPV failure of the base case and that of mitigation cases.

Table V shows delayed RPV failure time compared to base cases. For the SBLOCA, opening one ADV as a mitigation strategy significantly delayed RPV failure time by about 24 hours. This is attributed to the effective

cooling through secondary sides. The most delayed RPV failure time occurred when a mitigation strategy was conducted at CET = 923 K, which is the current SAMG entry condition of the OPR1000. For the SBO and TLOFW, opening SDS as a mitigation strategy delayed RPV failure time by about 2.4 and 13 hours, respectively. Since cooling through the secondary side was very inefficient, RPV failure time occurred relatively earlier than the SBLOCA mitigation cases. The most delayed RPV failure time took place when a mitigation strategy was conducted at CET = 923 K for the SBO and at CET = 753 K for the TLOFW. No consistent trend of the relationship between SAMG entry condition and RPV failure time was observed. It should be noted that earlier operator action or current SAMG entry conditions might not always yield the best result.

Table V: Delayed RPV failure time by mitigation strategy.

CET as SAMG entry condition (K)	SBLOCA (hr)	SBO (hr)	TLOFW (hr)
753	19.54	2.24	12.97
838	19.78	1.98	6.03
923	23.57	2.89	6.05
973	16.43	2.40	12.30

As presented in Table V, a current, unified SAMG entry condition might not produce the most desirable result in terms of delaying RPV failure. This is because the diagnosis of a severe accident is based on the symptoms of the plant. The symptom-based diagnosis is simply conducted by monitoring plant safety parameters such as CET, pressurizer pressure, SG water level, and so on. Therefore, the symptom-based diagnosis has advantages compared to an event-based diagnosis in terms of the availability of an operator's quick response. Most IAEA member states prefer to use the symptom-based diagnosis for severe accidents because severe accidents have characteristics of limited availability of monitoring parameters and accompany a dramatic and rapid change in phenomena such as core degradation, oxidation, and hydrogen generation [5]. Nonetheless, if symptom-based diagnosis is unable to produce the desirable result, it is necessary to consider use of event-based diagnosis for severe accidents.

Mass balance analysis for RCS has been performed to investigate the effect of SIT injection on the delayed RPV failure time associated with the CET of SAMG entry points. The pressures of the pressurizer and SIT were calculated, and cumulative mass injected to and from the RCS was also calculated. For all three accident scenarios, injection to the RCS originates from the SIT, but the ejection path has multiple possibilities. For the SBLOCA, the break in the cold leg is the only path for water ejection. In the cases of the SBO and TLOFW, however, paths for water ejection are the PSRV and SDS. Figs 3, 4 and 5 show the detailed pressure and corresponding mass balance of the SBLOCA-923K, SBO-923K, and TLOFW-753K, respectively.

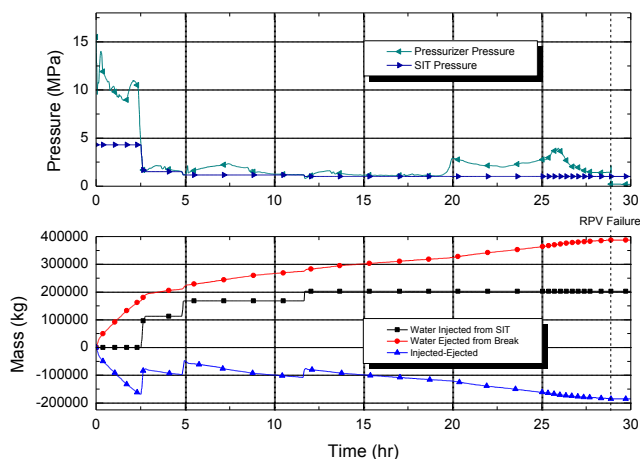


Fig. 3. Pressure behavior and cumulative water mass injected and ejected regarding RCS for SBLOCA-923K, the most delayed RPV failure time case.

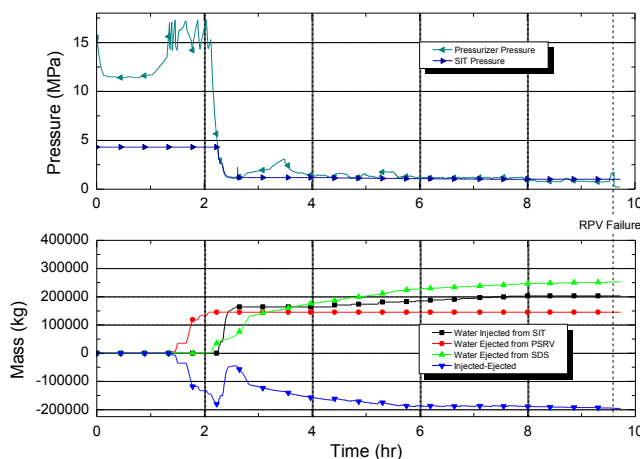


Fig. 4. Pressure behavior and cumulative water mass injected and ejected regarding RCS for SBO-923K, the most delayed RPV failure time case.

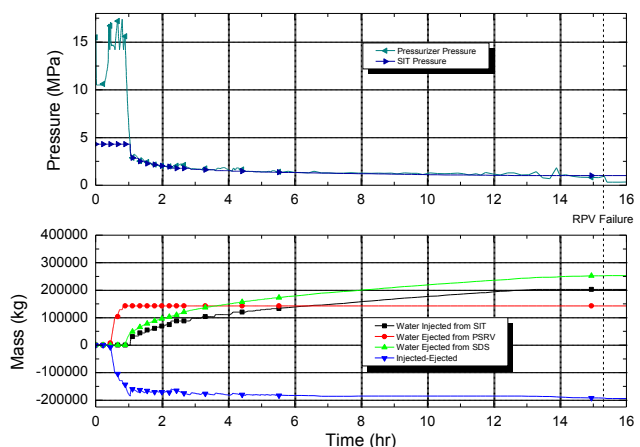


Fig. 5. Pressure behavior and cumulative water mass injected and ejected regarding RCS for TLOFW-753 K, the most delayed RPV failure time case.

Through the analysis, it was found that SIT injection played an important role in delaying the RPV failure. Thus, the timing and duration of the SIT injection were investigated thoroughly, from which an average SIT injection rate was estimated to explain its effect on the delayed RPV failure time. The average SIT injection rate is defined as the total mass of SIT injected over the actual duration of the SIT injection and is given in Eq. (1). Fig. 6 shows the relationship between average SIT injection rate and delayed RPV failure time. The lower injection rate of the SIT (in particular lower than 20 kg/s) resulted in a dramatic delaying of the RPV failure time. Note that the amount of borated water in the SIT inventory is fixed, and exhaust of the SITs differs with the accident scenario and is particularly dependent of the RCS pressure. In cases of SBLOCA with the explored SAMG entry conditions, injection rate varied from approximately 5 to 80 kg/s. The SBLOCA-923K, which showed the lowest SIT injection rate, resulted in the most delayed RPV failure time. As the SIT injection rate increased, the delayed RPV failure time decreased at an injection rate of 18 kg/s and slightly increased at an injection rate of approximately 80 kg/s. In cases of the SBO with the selected CET set points, the best mitigation result was obtained with CET = 923 K. A corresponding SIT injection rate was evaluated to be approximately 20 kg/s. Interestingly, the best mitigation result for the TLOFW was obtained when the CET was set to 753 K, which is the CET used for the CEOG SAMG entry point. The corresponding SIT injection rate recorded the lowest value of 5 kg/s. It should be noted that SIT injection rate was not controlled in the current study as the main interest was the effect of the CET and the resulting influence of the SIT injection rate. Thus, the SIT injection rate was investigated to support the CET effect from the analysis. From this analysis, a general trend was observed that a lower injection rate tended to provide a more effective cooling considering the fixed borated water mass in the SIT. Also, it is important to use all the borated water mass during accident management even though the current OPR1000 does not include control of the injection rate. As shown clearly in Figures 7 and 9, SIT was injected in a step-wise fashion due to vaporization of the core.

$$\text{Average SIT injection rate} = \frac{\text{Total injected water mass from SIT [kg]}}{\text{Actual duration of SIT injection [second]}} \quad (1)$$

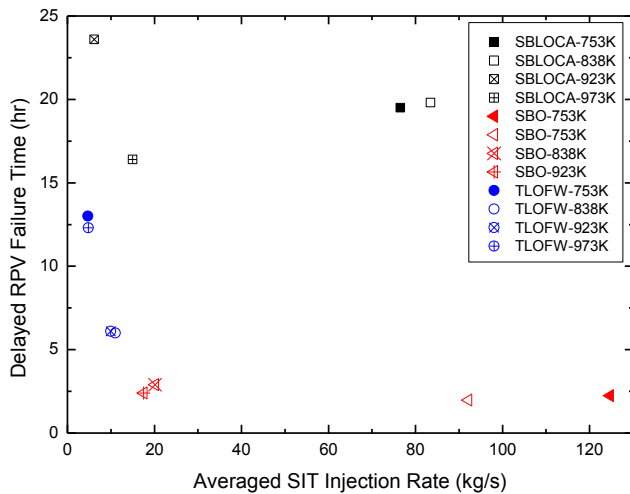


Fig. 6. Delayed RPV failure time dependent on the averaged SIT injection rate

3. Conclusion

The effectiveness of SAMG entry conditions for the postulated severe accident scenarios was analyzed with the MELCOR 1.8.6. First, SBLOCA, SBO, and TLOFW with mitigation strategies were investigated in terms of delaying RPV failure. The performance of mitigation strategies with four SAMG entry conditions (the time when CET=753, 838, 923 and 973 K) was analyzed. The most delayed RPV failure time occurred with different SAMG entry conditions for different scenarios. Therefore, it is imperative to consider using event-based diagnosis for severe accidents in further detailed studies. Second, Lower injection rate of SIT resulted in more delayed RPV failure time. In particular, SIT injection rates lower than 20 kg/s dramatically increased the delay in RPV failure time.

4. Acknowledgements

This work was supported by National Research Foundation of Korea (NRF) grants funded by MISP, grant numbers NRF-2012M2B2A6029184 and NRF-2014M2A8A4021295.

REFERENCES

- [1] Seongnyeon Lee et al., Validation of RCS depressurization strategy and core coolability map for independent scenarios of SBLOCA, SBO, and TLOFW, *Journal of Nuclear Science and Technology*, Vol. 51, p. 181-195, 2013.
- [2] R. Gauntt, R. Cole, S. Hodge, S. Rodriguez, R. Sanders, R. Smith, D. Stuart, R. Summers, M. Young. MELCOR computer code manuals: Division of Systems Technology, Office of Nuclear Regulatory Research, US Nuclear Regulatory Commission, Washington, DC (United States), 1998, Report no. NUREG/CR-6119
- [3] R-J Park, K-H Kang, K-S Ha, Y-R Cho, K-M Koo, S-B Kim, H-D Kim. Detailed analysis of a severe accident progression for an evaluation of in-vessel corium retention estimation in KSNP. Korea Atomic Energy Research Institute, Daejeon (Republic of Korea), 2005

[4] Korea Hydro and Nuclear Power. Shin Kori 1&2 Final Safety Analysis Report. Seoul (Korea): Korea Hydro and Nuclear Power; 2008.

[5] IAEA. Development and Review of Plant Specific Emergency Operating Procedures. Vienna (Austria): International Atomic Energy Agency; 2006